COMPUTER METHODS IN MATERIALS SCIENCE

2023, vol. 23, no. 2, 39–44
https://doi.org/10.7494/cmms.2023.2.0813

Viscoelastic characterization of additively manufactured acrylonitrile butadiene styrene

Szczepan Witek

AGH University of Krakow, al. A. Mickiewicza 30, 30-059 Krakow, Poland.

Abstract

The main objective of this work was to characterize the viscoelastic properties of additively manufactured Acrylonitrile Butadiene Styrene based on tensile stress relaxation tests. The stress relaxation measurements were conducted with a temperature range of 25–100°C. The two-layer viscoplastic constitutive model was adopted to describe the elastic and viscous behavior of the investigated material. The model parameters were calibrated using an inverse analysis and stress relaxation data. The model's predictive capabilities were assessed by comparing the model predictions with experimental data not included in the calibration process.

Keywords: fused filament fabrication, two-layer viscoplastic model, stress relaxation, ABS

1. Introduction

Fused filament fabrication (FFF) is a type of additive manufacturing technology that involves heating a thermoplastic material to a semi-molten state and extruding it through a nozzle, depositing it layer by layer along a predetermined path based on the desired part's geometry. The specific nature of such technology causes the mechanical behavior of additively manufactured parts to be strongly dependent on the parameters used in the process. Over the years, considerable experimental research has been conducted to investigate the influence of FFF process parameters on the mechanical behavior of printed parts. For example, Webbe Kerekes et al. (2019) evaluated the effects of infill density and layer thickness on the mechanical properties of ABS-M30 including Young's modulus, initial yield stress, ultimate strength, modulus of toughness, and elongation at break. Hanon et al. (2020) investigated the impact of build orientation, raster orientation, and layer thickness on the tensile strength and hardness properties of PLA. Extensive research was conducted by Hikmat et al. (2021). They examined the influence of build orientation, raster orientation, nozzle diameter, extruder temperature, infill density, number of contour lines, and extruding speed on the tensile strength of PLA.

In addition to the aforementioned mechanical properties, an important issue in the FFF process is obtaining a component without any distortion related to the level of residual stress (Casavola et al., 2017). These stresses are generated in the additively manufactured component as a result of repeated cycles of depositing a hotter layer on top of the previous partially cooled layer. High values of residual stresses can lead to part distortion or layer delamination during the printing process itself or in the final component. Similarly to the mechanical properties, the residual stresses

Author's email: switek@agh.edu.pl
ORCID ID: 0000-0002-4545-1863

are influenced by the FFF process parameters (Samy et al., 2022). The number of possible print parameter configurations is large, making experimental research time-consuming and expensive. Therefore, experimental research is supported or even replaced by numerical simulations based on the finite elements method (Gonabadi et al., 2021).

In order to perform a numerical simulation of the FFF process with adequate accuracy, the thermoplastic material should be characterized using an appropriate constitutive model. The thermoplastic materials used in the FFF process exhibit viscoelastic behavior such as stress relaxation and creep (Guedes et al., 2017). In existing works on 3D printing simulation, the influence of the viscoelastic behavior of the material, especially the influence of stress relaxation on residual stress, is generally neglected (Cattenone et al., 2019; Yang & Zhang, 2018).

Therefore, this work aims to characterize the elastic and viscous properties of Acrylonitrile Butadiene Styrene using the two-layer viscoplastic constitutive model built-in in the commercial finite element software Abaqus. In future work, the model will be used to simulate the FFF process to assess the influence of stress relaxation on residual stresses and distortion in additively manufactured parts.

2. Material and methods

2.1. Material and sample preparation

Commercial Acrylonitrile Butadiene Styrene (ABS) produced by Prusa was selected as investigated material. The non-standard test samples with the dimensions shown in Figure 1a were used for the stress relaxation tests. The samples were additively manufactured on a Prusa i3 MK3s printer with a layer thickness of 0.2 mm and 100% infill density. The FFF process was carried out at the extruder temperature of 240°C. The table temperature was 100°C and 110°C for the first and other layers, respectively. The raster angle in the measuring zone of the sample was equal to 0° (Fig. 1b).

2.2. Tension relaxation tests

The stress relaxation tests were performed on a specially constructed machine. The force was measured using an Axis FB200 dynamometer with a maximum load of 200 N. An electric mini-furnace equipped with two electric heaters was used as a heating device. The temperature in the furnace was controlled using On/Off temperature controller. A type K thermocouple was used to monitor the temperature in the furnace. The strain was measured using an optical measurement method based on two dots tracking. The distance between the dots was 20 mm. The tests were performed in the elastic range. The general view of the setup used in the experiment is shown in Figure 2.

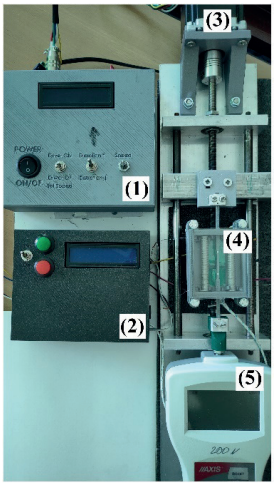

Fig. 2. Stress relaxation test equipment: 1) power block; 2) On/Off temperature controller, 3) electric motor; 4) furnace with sample; 5) Axis FB200 dynamometer

The stress relaxation tests were carried out at temperatures of 25, 40, 60, 80, 90 and 100°C. The time of heating the sample to the test temperature was determined using FEM analysis and was equal to 20 min. During the test, the sample was uniaxially stretched to a target strain value of 0.015 at a constant cross-head speed rate of 0.02 mm/s, while force and strain were recorded. The test time was set at 20 min. For each temperature variant, three measurements were made.

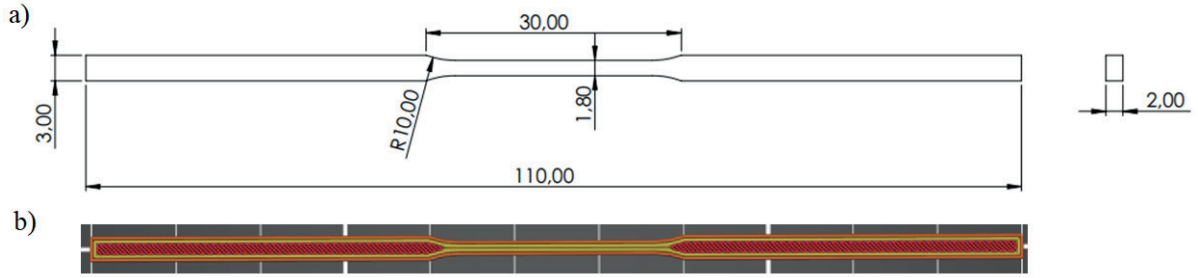

Fig. 1. Stress relaxation test sample: a) dimensions [mm]; b) raster angle

In order to assess the predictive capabilities of the model, two additional stress relaxation measurements were performed at temperatures 75°C and 85°C.

2.3. Viscoplastic model

The viscoelastic characterization of the investigated material was carried out using the two-layer viscoplastic constitutive model (TLVP). The TLVP model is implemented in Abaqus and is widely used for modeling materials in which time-dependent phenomena, as well as plasticity, are observed (Doh et al., 2018). The model consists of an elastic-plastic network that is in parallel with an elastic-viscous network, as shown in Figure 3. Thus, the model consists of an elastic, plastic, and viscous part. Due to the parallel configuration, the total stress is the sum of the stresses of elastic-plastic and elastic-viscous networks.

The elastic part for both networks is defined using a linear isotropic elasticity model, and the networks are related by parameter f according to the equation:

$$f = \frac{K_v}{K_p + K_v} \tag{1}$$

In Equation (1) f denotes the ratio of the elastic modulus of the elastic-viscous network (K_v) to the total (instantaneous) modulus:

$$K = K_p + K_v \tag{2}$$

In the elastic-plastic network shown in Figure 3, K_p denotes the elastic modulus, H is the plastic hardening modulus, and σ_y is the yield stress.

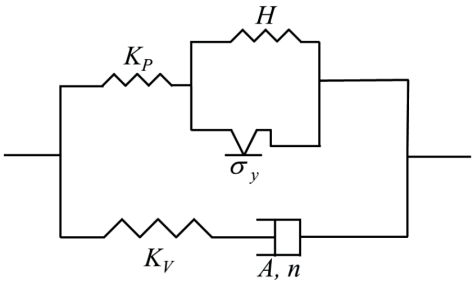

Fig. 3. One-dimensional idealization of the two-layer viscoplastic model

The plastic behavior of the material can be characterized by any of the available Abaqus metal plasticity models. The limitation of the two-layer viscoplastic model is that the elastic-plastic network does not take into account rate-dependent yield. In the current work, the plastic part of the elastic-plastic network was neglected.

The viscous behavior of the elastic-viscous network was assumed to be governed by the Norton–Hoff creep law:

$$\dot{\tilde{\varepsilon}}^{er} = A\tilde{\sigma}^n \tag{3}$$

where: $\dot{\tilde{\varepsilon}}^{er}$ – the uniaxial equivalent creep strain rate; A, n – Norton–Hoff rate parameters; $\tilde{\sigma}$ – Mises equivalent stress.

2.4. Identification of model parameters

Four parameters A, n, f, K of the two-layer viscoplastic constitutive model have to be identified to completely characterize the investigated materials. This can be accomplished using an inverse analysis method rely on minimizing a properly defined objective function with respect to unknown parameters (Zhang et al., 2014). The scheme of an inverse algorithm is shown in Figure 4. The inverse analysis algorithm consists of three main parts, i.e. experiment, simulation, and optimization. The solution is found iteratively using an appropriate optimization algorithm to minimize the objective function which is defined for quantifying the difference between experimental and simulated results. For the case under consideration, the objective function ϕ can be formulated as a root mean square error (RMSE) between the stresses obtained from the measurements (σ^m) and numerical calculations (σ^c):

$$\phi(A,n,f,K) = \sqrt{\frac{\sum_{i=1}^{w}(\sigma_i^m - \sigma_i^c)^2}{w}} \tag{4}$$

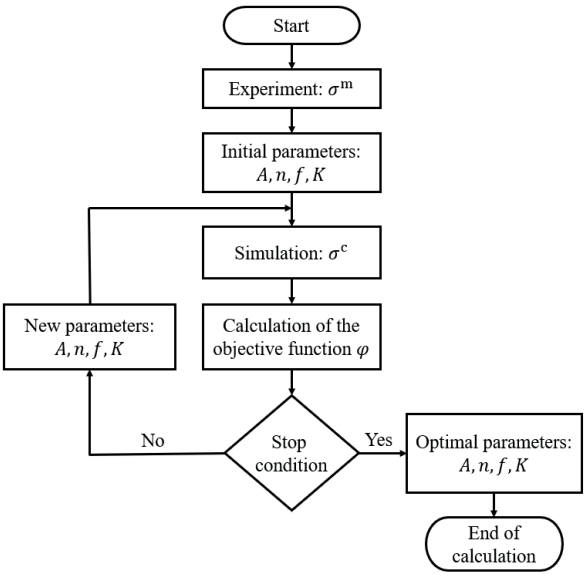

Fig. 4. Inverse analysis algorithm

In recent years, when determining material parameters through inverse analysis, the term simulation is most often understood as a simulation made with the use of the finite element method (Rauchs & Bardon, 2011). The main drawback of this approach is the long calculation time, even when only one single finite element is used (Berezvai & Kossa, 2020). A solution to this problem was proposed in work (Kossa & Horváth, 2021), where the simulation with the finite element method was replaced by the solution that relied on numerical integration of the two-layer viscoplastic constitutive model. The authors of that work used the implicit midpoint integration scheme applied on the elastic-viscous network. For the purposes of this work, the proposed numerical solution was implemented in Visual Basic as an additional module of Microsoft Excel. Optimization was performed using the Solver add-in and the Generalized Reduced Gradient (GRG) method (Lasdon et al., 1974). The stop condition was defined as the absolute value of the relative change in the objective function being less than 0.0001 for the last 5 consecutive iterations. The following constraints for the parameters were adopted: $A, n, K > 0$, and $0 < f < 1$. A scaling factor of 10^{-6} and 10^{3} was used for A and K parameters, respectively. The initial parameter values were 10^{-6}, 4, 0.6, 1.5 for A, n, f, and K respectively. The two-layer viscoplastic constitutive model parameters were identified from the tension relaxation tests.

3. Results

A comparison of experimental and prediction stress relaxation curves for all tested temperatures is presented in Figure 5. The calibrated TLVP model parameters for ABS material are listed in Table 1. The data included in the table were averaged from three measurements, and the relative standard deviation was provided to evaluate the repeatability of the stress relaxation tests. The observed decrease in total elastic modulus (K) with increasing temperature is consistent with the results reported by Li et al. (2020). At 25°C and 100°C, the elastic modulus is 1542 MPa and 240 MPa, respectively. According to the provided data, the relative standard deviation for the elastic modulus is relatively low, ranging from 0.91% to 5.93%. The viscoelastic parameters f and A increase as temperature increases. This indicates that ABS material becomes more viscoelastic, exhibiting greater time-dependent behavior at higher temperatures. The relative standard deviation for the parameter f is low, ranging from 0.27% to 2.64%. In all cases, the RMSE value is very low, which confirms a very good fit of the TLVP model to the experimental data. The obtained relative standard deviation results for parameters K and f indicate that the performed stress relaxation tests produce repeatable results.

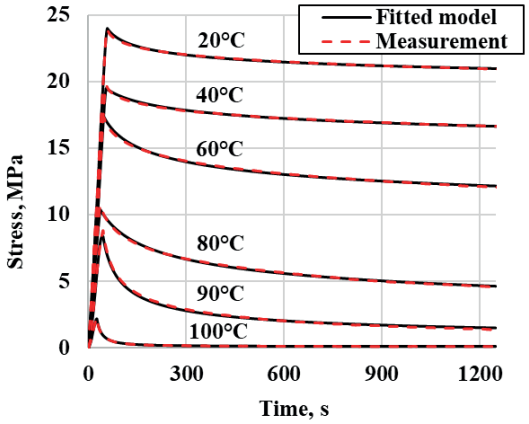

Fig. 5. A comparison of stress relaxation measurement data used in the calibration procedure with the fitted TLVP model

The non-linear dependence of parameters K, f, A, and n on temperature is depicted in Figure 6. The presented data show that the parameter A increases exponentially with increasing temperature, therefore it was approximated by the exponential function described by Equation (5). The other parameters were approximated by polynomial function according to Equation (6).

$$A(\theta) = A_{25} \exp\left(a_1\theta^4 + a_2\theta^3 + a_3\theta^2 + a_4\theta\right) \tag{5}$$

$$n(\theta), f(\theta), K(\theta) = a_1\theta^3 + a_2\theta^2 + a_3\theta + a_4 \tag{6}$$

$$\theta = \frac{T - 25}{100} \tag{7}$$

where: $a_1 - a_4$ – empirical coefficients; T – temperature.

Table 1. The average fitted parameters of the TLVP model for ABS material

T [°C]	K [MPa]	f	A	n	ϕ
25	1542.08 ±3.37%	0.302 ±2.64%	2.00E-11	7.7	0.068
40	1349.79 ±5.93%	0.387 ±1.39%	2.00E-11	7.1	0.072
60	1176.92 ±2.03%	0.613 ±1.47%	9.50E-11	5.75	0.089
80	749.52 ±5.70%	0.920 ±0.27%	6.52E-09	4.1	0.067
90	598.96 ±5.65%	0.981 ±1.73%	5.26E-07	2.94	0.075
100	240.22 ±0.91%	0.979 ±0.60%	1.49E-04	1.77	0.008

Table 2 presents the empirical coefficients obtained for Equations (5) and (6). These coefficients were subsequently used to calculate the stress relaxation curves at temperatures 75°C and 85°C, which were not used in the calibration procedure, to assess the predictive capabilities of the TLVP model. A comparison between experimental and calculated stress relaxation curves for the aforementioned temperatures is presented in Figure 7. The RMSE value for temperature variants 75°C and 85°C is equal to 0.139 and 0.614, respectively. For the temperature variant 85°C, the calculated relaxation curve slightly deviates from the experimental one. This can be explained by the results of the relative standard deviation of the model parameters, which are in the range of 0.27–5.93%. Changing the parameters of the TLVP model by ±3% causes the RMSE value to decrease from 0.614 to 0.22, and the curves fit very well (Fig. 7).

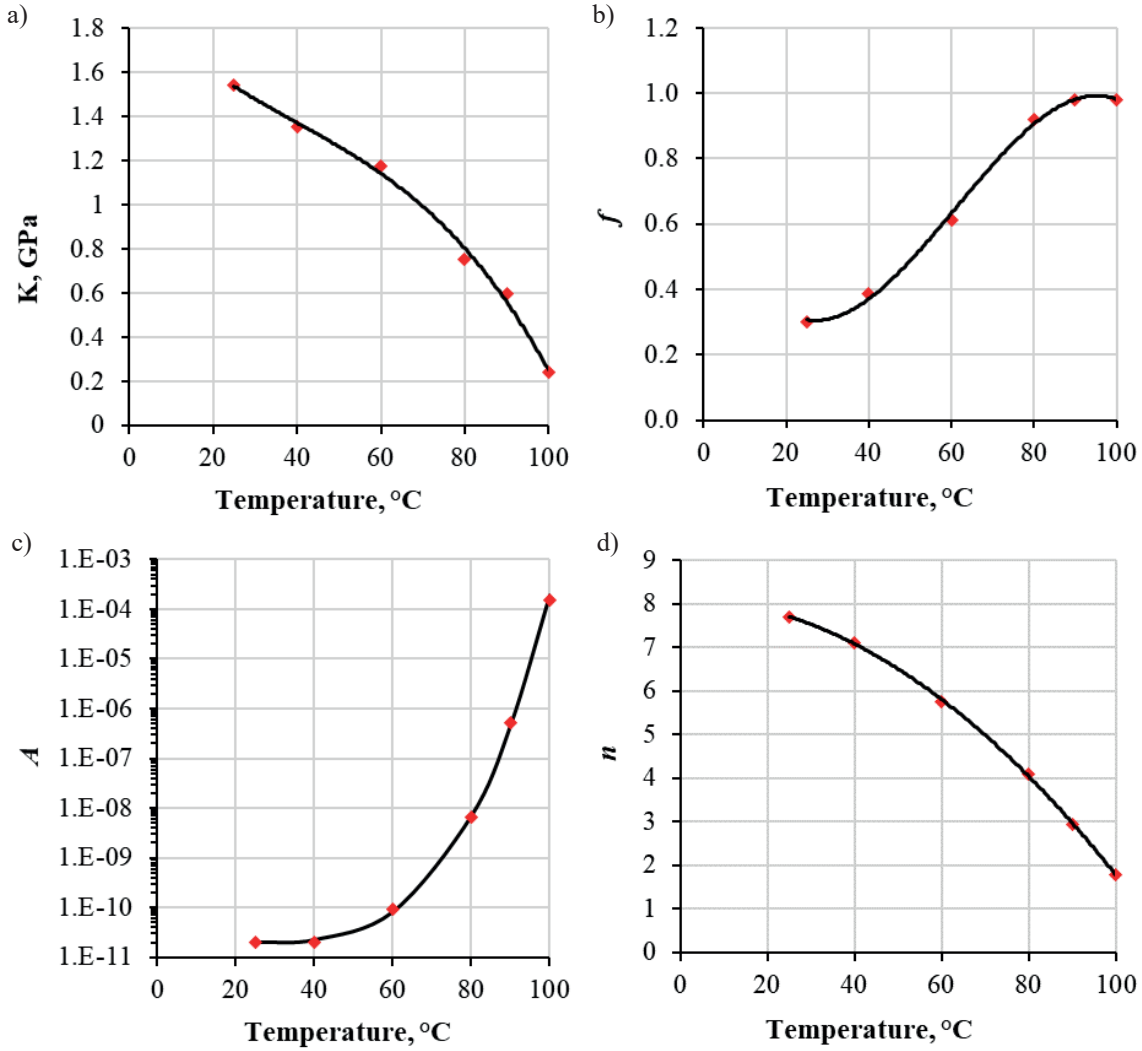

Fig. 6. The temperature dependence of TLVP model parameters: a) *K*; b) *f*; c) *A*; d) *n*

Table 2. The empirical coefficients for TLVP model parameters

	K	*f*	*A*	*n*
a_1	−2.209	−4.339	26.062	0
a_2	0.964	4.689	5.005	−6.191
a_3	−1.196	−0.177	12.167	−3.265
a_4	1.536	0.307	−1.794	7.705

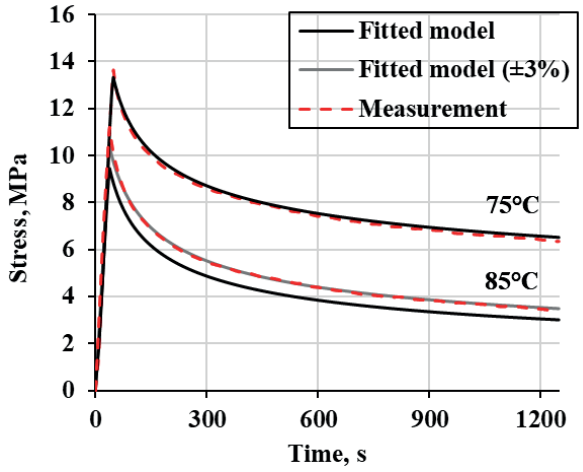

Fig. 7. A comparison of stress relaxation measurement data not used in the calibration procedure with the fitted TLVP model

4. Summary

This paper aimed to characterize the viscoelastic behavior of Acrylonitrile Butadiene Styrene using the two-layer viscoplastic constitutive model integrated into the finite element software Abaqus. The model was calibrated through tension relaxation tests and inverse analysis. The temperature-dependent parameters of the TLVP model were approximated using exponential and polynomial functions. The stress relaxation curves obtained experimentally were compared with the predicted curves for all tested temperatures. The agreement between the experimental and predicted curves indicates that the TLVP model can accurately describe the time-dependent behavior of the ABS material. In further research, the model will be used to examine the effect of stress relaxation on the residual stress level and distortions in FFF parts.

References

Berezvai, S., & Kossa, A. (2020). Performance of a parallel viscoelastic-viscoplastic model for a microcellular thermoplastic foam on wide temperature range. *Polymer Testing*, *84*, 106395. https://doi.org/10.1016/j.polymertesting.2020.106395.

Casavola, C., Cazzato, A., Moramarco, V., & Pappalettera, G. (2017). Residual stress measurement in Fused Deposition Modelling parts. *Polymer Testing*, *58*, 249–255. https://doi.org/10.1016/j.polymertesting.2017.01.003.

Cattenone, A., Morganti, S., Alaimo, G., & Auricchio, F. (2019). Finite element analysis of additive manufacturing based on fused deposition modeling: Distortions prediction and comparison with experimental data. *Journal of Manufacturing Science and Engineering*, *141*(1), 011010. https://doi.org/10.1115/1.4041626.

Doh, J., Hur, S.H., & Lee, J. (2018). Viscoplastic parameter identification of temperature-dependent mechanical behavior of modified polyphenylene oxide polymers. *Polymer Engineering and Science*, *59*(S1), E200-E211. https://doi.org/10.1002/pen.24910.

Gonabadi, H., Chen, Y., Yadav, A., & Bull, S. (2022). Investigation of the effect of raster angle, build orientation, and infill density on the elastic response of 3D printed parts using finite element microstructural modeling and homogenization techniques. *The International Journal of Advanced Manufacturing Technology*, *118*, 1485–1510. https://doi.org/10.1007/s00170-021-07940-4.

Guedes, R.M., Singh, A., & Pinto, V. (2017). Viscoelastic modelling of creep and stress relaxation behaviour in PLA-PCL fibres. *Fibers and Polymers*, *18*(12), 2443–2453. https://doi.org/10.1007/s12221-017-7479-y.

Hanon, M.M., Dobos, J., & Zsidai, L. (2020). The influence of 3D printing process parameters on the mechanical performance of PLA polymer and its correlation with hardness. *Procedia Manufacturing*, *54*, 244–249. https://doi.org/10.1016/j.promfg.2021.07.038.

Hikmat, M., Rostam, S., & Ahmed, Y.M. (2021). Investigation of tensile property-based Taguchi method of PLA parts fabricated by FDM 3D printing technology. *Results in Engineering*, *11*, 100264. https://doi.org/10.1016/j.rineng.2021.100264.

Kossa, A., & Horváth, A.L. (2021). Powerful calibration strategy for the two-layer viscoplastic model. *Polymer Testing*, *99*, 107206. https://doi.org/10.1016/j.polymertesting.2021.107206.

Lasdon, L., Fox, R., & Ratner, M. (1974). Nonlinear optimization using the generalized reduced gradient method. *Informatique et Recherche Opérationn*, *3*, 73–103. https://doi.org/10.1051/ro/197408V300731.

Li, J., Jia, Y., Li, T., Zhu, Z., Zhou, H., Peng, X., & Jiang, S. (2020). Tensile Behavior of Acrylonitrile Butadiene Styrene at Different Temperatures. *Advances in Polymer Technology*, *2020*, 1–10. https://doi.org/10.1155/2020/8946591.

Rauchs, G., & Bardon, J. (2011). Identification of elasto-viscoplastic material parameters by indentation testing and combined finite element modelling and numerical optimization. *Finite Elements in Analysis and Design*, *47*(7), 653–667. https://doi.org/10.1016/j.finel.2011.01.008.

Samy, A.A., Golbang, A., Harkin-Jones, E., Archer, E., Dahale, M., McAfee, M., Abdi, B., & McIlhagger, A. (2022). Influence of Raster Pattern on Residual Stress and Part Distortion in FDM of Semi-Crystalline Polymers: A Simulation Study. *Polymers*, *14*(13), 2746. https://doi.org/10.3390/polym14132746.

Webbe Kerekes, T., Lim, H., Joe, W.Y., & Yun, G.J. (2019). Characterization of process–deformation/damage property relationship of fused deposition modeling (FDM) 3D-printed specimens. *Additive Manufacturing*, *25*, 532–544. https://doi.org/10.1016/j.addma.2018.11.008.

Yang, H., & Zhang, S. (2018). Numerical simulation of temperature field and stress field in fused deposition modeling. *Journal of Mechanical Science and Technology*, *32*(7), 3337–3344. https://doi.org/10.1007/s12206-018-0636-4.

Zhang, W., Cho, C., & Xiao, Y. (2014). An effective inverse procedure for identifying viscoplastic material properties of polymer Nafion. *Computational Materials Science*, *95*, 159–165. https://doi.org/10.1016/j.commatsci.2014.07.033.